



## NON-LINEAR COUPLED SLOSH DYNAMICS OF LIQUID STORAGE TANKS USING BE-FE COUPLING

M.K. KIM<sup>1</sup>, Y.M. LIM<sup>2</sup>, K.H. CHO<sup>3</sup>, I.H. YANG<sup>4</sup> and J. EO<sup>5</sup>

### SUMMARY

An analysis program for the base isolated liquid storage tank was developed considering non-linear fluid-structure interaction in this study. The behavior of a fluid region is simulated by the boundary element method and the analysis scheme of the free surface motion in time domain is developed by using the nonlinear free surface boundary condition(NFBC). In order to construct the governing equation of the whole system, finite elements for a structure and boundary elements for a fluid region are coupled using the equilibrium and compatibility conditions and NFBC. The isolator is simulated by equation proposed in 3D Basis Me.

Some numerical examples are presented to demonstrate the validity and the applicability of the developed procedure. The forced vibration analysis demonstrates that the developed method can represent the large sloshing motion of free surface well. Then, the dynamic analysis of liquid storage tank is performed to study the effect of the NFBC and the results are compared. Finally, the applicability of the developed method is verified through the seismic analysis of a real size liquid storage tank for the artificial earthquake.

### INTRODUCTION

The dynamic response of liquid storage tanks under seismic ground motion is different from that of common structures such as buildings or bridges. It is well known that the difference of the response is caused by the effect of the fluid-structure interaction. Thus, to predict the behavior of the container, the distribution of hydrodynamic pressure and the fluid sloshing motion should be evaluated reasonably. Especially, in case of wave propagation of long period earthquake or introduction of the base isolation system for reducing the damage due to a seismic motion, the sloshing height can be amplified thoughtfully. Excessive sloshing height may cause the unexpected pressure on the connection of roof-wall

---

<sup>1</sup> Professor, Yonsei University, Seoul, Korea. Email: applymkk@yonsei.ac.kr

<sup>2</sup> Assistant Professor, Yonsei University, Seoul, Korea.

<sup>3</sup> Graduate Student, Yonsei University, Seoul, Korea.

<sup>4</sup> Senior Researcher, Daelim Industrial Co., Ltd., Seoul, Korea.

<sup>5</sup> Researcher, Daelim Industrial Co., Ltd., Seoul, Korea.

and spillage of contained liquid. When the large sloshing motion occurs, it is needed to consider the nonlinear free surface boundary condition (NFBC).

In this study, a numerical algorithm, which can analyze the fluid-structure interaction problem considering the NFBC, is developed and the corresponding dynamic responses of base isolated liquid storage tanks are investigated. The behavior of a fluid region is simulated by boundary elements and a structure region is modeled by finite elements in three dimensional coordinate. The isolator system is modeled by equation proposed in 3D Basis Me. Then, the NFBC is imposed on the free surface of a fluid region and the interaction effect is simulated directly by transferring the normal acceleration of structure to the fluid domain and the hydrodynamic pressure to the structure domain at the fluid-structure interface. Through these procedures, the response of the base-isolated liquid storage tank considering non-linear behavior of free surface is analyzed combining the three parts by FE-BE coupling.

## FORMULATION FOR FLUID AND STRUCTURE REGIONS

### Modeling of a fluid region

In this study, for the simplicity, the contained liquid is assumed to be inviscid and incompressible, resulting in an irrotational flow field. In view of these assumptions, the governing equation of the liquid motion is represented as follows

$$\nabla^2 \phi(\mathbf{x}, t) = 0 \quad (1)$$

where  $\phi$  is the velocity potential and  $\mathbf{x} = (x, y, z)$  is the position vector. Eq. (1) is the Laplace equation and the boundary integral equation derived from Lagrange-Green Identity can be written as

$$c(\xi, t)\phi(\xi, t) = \int_{\Gamma} \phi^*(\xi, \mathbf{x}, t) \frac{\partial \phi(\xi, t)}{\partial \mathbf{n}} d\Gamma - \int_{\Gamma} \frac{\partial \phi^*(\xi, \mathbf{x}, t)}{\partial \mathbf{n}} \phi(\xi, t) d\Gamma \quad (2)$$

where  $\Gamma$  is the boundary of a fluid region,  $\mathbf{n}$  is normal vector,  $\xi$  is the source point,  $\mathbf{x}$  is the receive point and  $\phi^*(\xi, \mathbf{x}, t)$  is the fundamental solution of Laplace equation or Green function.

To integrate the obtained boundary integral equation numerically, the boundary surface is discretized into a series of elements and nodes. Then, using the boundary element technique, Eq. (2) can be expressed in matrix form as

$$\mathbf{H}\phi = \mathbf{G} \frac{\partial \phi}{\partial \mathbf{n}} \quad (3)$$

where  $\mathbf{H}$  and  $\mathbf{G}$  are boundary element coefficient matrices for the potential vector  $\phi$  and the flux vector  $\frac{\partial \phi}{\partial \mathbf{n}}$ , respectively.

When a liquid storage tank is subjected to a dynamic load, the boundary conditions on the free surface are obtained by formulating the dynamic and kinematic boundary conditions. The dynamic boundary condition is that the pressure on the free surface must be equal to the atmospheric pressure and the kinematic boundary condition is that liquid particles which are on the free surface remain on it during

subsequent motion. The dynamic boundary condition assuming the atmospheric pressure to be zero is expressed as

$$\frac{\partial \phi(\mathbf{x}, t)}{\partial t} + \frac{1}{2} \nabla \phi \nabla \phi + g \eta(x, y, t) = 0 \quad (4)$$

where  $\eta(x, y, t)$  is the sloshing height,  $g$  is the gravitational acceleration. The kinematic boundary condition is expressed as follows.

$$\frac{Dx_f}{Dt} = \nabla \phi \quad (5)$$

At the interface between liquid and the tank wall, the normal component of the liquid velocity is equal to the velocity of tank wall. Then the boundary condition is expressed as

$$\frac{\partial \phi(\mathbf{x}, t)}{\partial \mathbf{n}} = v_n(t) \quad (6)$$

where  $v_n(t)$  is the velocity normal to the surface of the tank wall. The hydrodynamic pressure acting on the wall (Eq. (8)) can be derived from Eq. (7).

$$\frac{\partial \phi(\mathbf{x}, t)}{\partial t} + \frac{P(\mathbf{x}, t)}{\rho_l} + \frac{1}{2} \nabla \phi \nabla \phi + g \eta(x, y, t) = F(t) \quad (7)$$

$$P(\mathbf{x}, t) = -\rho_l \frac{\partial \phi(\mathbf{x}, t)}{\partial t} - \frac{1}{2} \rho_l \nabla \phi \nabla \phi \quad (8)$$

Where  $\rho$  is the liquid density.

### Modeling of a structure region

The structure domain is modeled using 9-noded degenerated shell elements with five degrees of freedom per node. The discretized form of the governing equation of motion subjected to seismic ground excitation for the liquid-structure system is written as

$$\mathbf{M}^s \ddot{\mathbf{u}} + \mathbf{C}^s \dot{\mathbf{u}} + \mathbf{K}^s \mathbf{u} = \mathbf{R}(t) \quad (9)$$

where  $\mathbf{M}^s$ ,  $\mathbf{C}^s$  and  $\mathbf{K}^s$  are the mass matrices, the Rayleigh damping matrices and the stiffness matrices of the structure, respectively. Also,  $\ddot{\mathbf{u}}$ ,  $\dot{\mathbf{u}}$ , and  $\mathbf{u}$  are the nodal accelerations, velocities, and displacements of the structure, respectively. Superscript  $s$  denotes the matrix for a structure region.  $\mathbf{R}(t)$  is the force vector for seismic ground excitation and for the fluid-structure interaction system, written as

$$\mathbf{R}(t) = -\mathbf{M}^s \mathbf{r} \ddot{\mathbf{u}}_g(t) + \mathbf{f}(t) \quad (10)$$

where  $\ddot{\mathbf{u}}_g$  is the ground acceleration vector in time domain and  $\mathbf{r}$  is transformation vector that couples each degree of freedom to the ground motion.  $\mathbf{f}(t)$  represents the nodal forces exerted on the container wall due to pressure arising from the oscillation of the liquid.

### Modeling of the base isolation system

The base isolation system, presented by Tsopelas, P.C., et. al. [5], is applied in this study. The forces along the orthogonal directions mobilized during motion of elastomeric bearings are described by

$$F_x = \alpha \frac{F^y}{y} U_x(t + \Delta t) + (1 - \alpha) F^y Z_x, \quad F_y = \alpha \frac{F^y}{y} U_y(t + \Delta t) + (1 - \alpha) F^y Z_y \quad (11)$$

where  $\alpha$  is the post-yielding to pre-yielding stiffness ratio,  $F^y$  is the yield force and  $Y$  is the yield displacement, as illustrated in Fig. 1.  $Z_x$  and  $Z_y$  are dimensionless variables governed by the following system of differential equations proposed by Park, et al. [6].

$$\begin{cases} \dot{Z}_x Y \\ \dot{Z}_y Y \end{cases} = \begin{cases} A \dot{U}_x \\ A \dot{U}_y \end{cases} - \begin{bmatrix} Z_x^2 (\gamma \text{Sgn}(\dot{U}_x Z_x) + \beta) & Z_x Z_y (\gamma \text{Sgn}(\dot{U}_y Z_y) + \beta) \\ Z_x Z_y (\gamma \text{Sgn}(\dot{U}_x Z_x) + \beta) & Z_y^2 (\gamma \text{Sgn}(\dot{U}_y Z_y) + \beta) \end{bmatrix} \begin{cases} \dot{U}_x \\ \dot{U}_y \end{cases} \quad (12)$$

Where  $A$ ,  $\lambda$  and  $\beta$  are dimensionless qualities that control the shape of the hysteretic loop. The values of  $A=1$ ,  $\lambda=0.9$  and  $\beta=0.1$  are used in this paper.  $Z_x$  and  $Z_y$  are acquired by adopting the following fourth-order Runge-Kutta method which is widely used in nonlinear dynamic analysis programs and rapidly converge to the correct solution when the nonlinearities of system are mild.

$$Z_{i+1} = Z_i + \left[ \frac{1}{6} (K_1 + 2K_2 + 2K_3 + K_4) \right] \Delta T \quad (13)$$

where

$$K_1 = f(T_i, Z_i), \quad K_2 = f\left(T_i + \frac{1}{2} \Delta T, Z_i + \frac{1}{2} K_1 \Delta T\right),$$

$$K_3 = f\left(T_i + \frac{1}{2} \Delta T, Z_i + \frac{1}{2} K_2 \Delta T\right), \quad K_4 = f(T_i + \Delta T, Z_i + K_3 \Delta T)$$

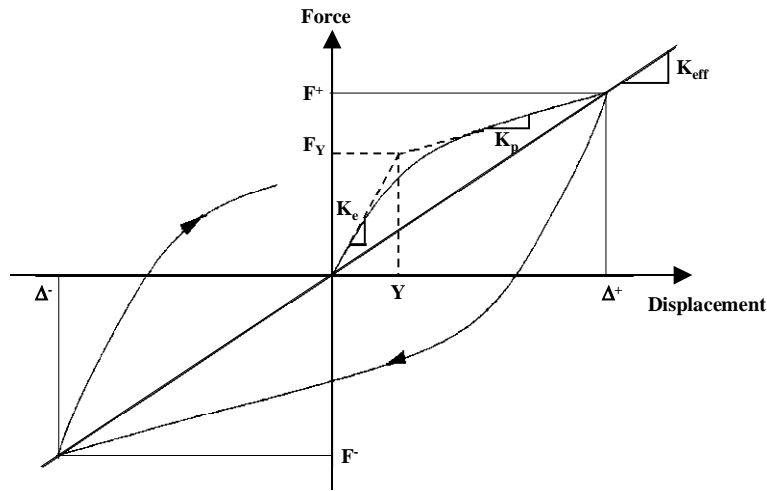


**Fig. 1 Force-displacement diagram for isolation system**

## DYNAMIC ANALYSIS OF FLUID-STRUCTURE-BASE ISOLATION INTERACTION

### Solution procedure of non-linear sloshing motion

To predict the non-linear behavior of free surface numerically, the Lagrangian particle approach is used. The Lagrangian particle approach introduces the procedure that the free surface is composed of a group of fluid particles which move in a Lagrangian manner at every time step.

In this procedure, potential  $\phi^{k+1}$  at the k+1-th time step can be determined from the fluid particle potential  $\phi^k$  and  $(D\phi/Dt)^k$  by using the boundary conditions, Eq. (5), Eq. (6) and the Lagrangian form of Eq. (4) at the k-th time step. Although there exist various kinds of scheme, the following Euler scheme known as the simplest time integration method is adopted.

$$\phi^{k+1} = \phi^k + (D\phi/Dt)^k \Delta t \quad (14)$$

Where  $\Delta t$  denotes the short time interval. Under this potential  $\phi^{k+1}$ , Eq. (3) can be solved and the flux values  $(\partial\phi/\partial\mathbf{n})^{k+1}$  can be obtained on a free surface. By using these potential gradients, fluid particle velocity is calculated and then the new value of the fluid particle position at the k+1-th time step is determined. From above procedures, the initial values for a fluid region at the start of the next time step can be obtained. Also, a new boundary element mesh is generated corresponding to the updated geometry.

### Coupling of whole governing equations

To solve the discretized governing equation of a fluid region in time domain, Eq. (3) is differentiated about time and divided into a free surface region and a fluid-structure interface region. Then, substituting Eqs. (4)-(8) into the partitioned Eq. (3) leads to the following,

$$\frac{1}{\rho} \begin{bmatrix} \mathbf{H}_{pp} & \mathbf{H}_{p\eta} \\ \mathbf{H}_{\eta p} & \mathbf{H}_{\eta\eta} \end{bmatrix} \left\{ \begin{array}{l} \mathbf{P}_p + \rho \cdot \mathbf{A}_p \\ \rho \cdot \mathbf{g} \cdot \boldsymbol{\eta} + \rho \cdot \mathbf{A}_\eta \end{array} \right\} + \begin{bmatrix} \mathbf{G}_{pp} & \mathbf{G}_{p\eta} \\ \mathbf{G}_{\eta p} & \mathbf{G}_{\eta\eta} \end{bmatrix} \left\{ \begin{array}{l} \mathbf{n} \cdot \ddot{\mathbf{u}}_p \\ \ddot{\boldsymbol{\eta}} \end{array} \right\} = \{\mathbf{0}\} \quad (15)$$

where,  $\boldsymbol{\eta}$ ,  $\ddot{\boldsymbol{\eta}}$  are the sloshing displacement and sloshing acceleration vectors,  $\ddot{\mathbf{u}}$ ,  $\mathbf{P}$  are the acceleration vector and hydrodynamic pressure vector at the interface between fluid and the structure, and  $\mathbf{n}$  is the outer normal vector.  $\mathbf{A}_p$  and  $\mathbf{A}_\eta$  are non-linear terms of fluid-structure interface and free surface, respectively and expressed as  $0.5\nabla\phi\nabla\phi$ . Subscript  $\eta$  and  $p$  denote the nodes for the free surface of liquid and the nodes on the fluid-structure interface, respectively.

Hydrodynamic pressure, shown in Eq. (16) and sloshing motion, shown in Eq. (17) can be expressed as functions of  $\ddot{\mathbf{u}}_p$ ,  $\boldsymbol{\eta}$ ,  $\ddot{\boldsymbol{\eta}}$ ,  $\mathbf{A}_p$  and  $\mathbf{A}_\eta$  by converting Eq. (15).

$$\mathbf{P}_p / \rho = -\mathbf{P}_1 \ddot{\mathbf{u}}_p - \mathbf{P}_2 \ddot{\boldsymbol{\eta}} - \mathbf{P}_3 \boldsymbol{\eta} - \mathbf{P}_4 \mathbf{A}_\eta - \mathbf{P}_5 \mathbf{A}_p \quad (16)$$

$$\mathbf{M}_{\eta p}^l \ddot{\mathbf{u}}_p + \mathbf{M}_{\eta\eta}^l \ddot{\boldsymbol{\eta}} + \mathbf{K}_{\eta\eta}^l \boldsymbol{\eta} + \mathbf{K}_{\eta\eta}^l \mathbf{A}_\eta = \mathbf{0} \quad (17)$$

Where,

$$\mathbf{P}_1 = \mathbf{n} \cdot \mathbf{H}_{pp}^{-1} \mathbf{G}_{pp}, \mathbf{P}_2 = \mathbf{H}_{pp}^{-1} \mathbf{G}_{p\eta}, \mathbf{P}_3 = g \mathbf{H}_{pp}^{-1} \mathbf{H}_{p\eta}, \mathbf{P}_4 = \mathbf{H}_{pp}^{-1} \mathbf{H}_{p\eta}, \mathbf{P}_5 = \mathbf{I}$$

$$\mathbf{M}_{\eta p}^l = \mathbf{n} \cdot [\mathbf{G}_{\eta p} - \mathbf{H}_{\eta p} \mathbf{H}_{pp}^{-1} \mathbf{G}_{pp}], \mathbf{M}_{\eta\eta}^l = \mathbf{G}_{\eta\eta} - \mathbf{H}_{\eta p} \mathbf{H}_{pp}^{-1} \mathbf{G}_{p\eta}, \mathbf{K}_{\eta\eta}^l = g \cdot [\mathbf{H}_{\eta\eta} - \mathbf{H}_{\eta p} \mathbf{H}_{pp}^{-1} \mathbf{H}_{p\eta}]$$

Superscript  $l$  denotes the matrix for the liquid region. To convert hydrodynamic pressure  $[\mathbf{P}_p]$  into the equivalent nodal force of the finite element  $[\mathbf{f}]$ , the shape function matrix used in finite element formulation,  $[\mathbf{N}]$  is introduced. Then, the hydrodynamic pressure, Eq. (16) can be expressed as follows:

$$\mathbf{f} = \mathbf{NP} = -\mathbf{NP}_1\ddot{\mathbf{u}}_p - \mathbf{NP}_2\ddot{\boldsymbol{\eta}} - \mathbf{NP}_3\boldsymbol{\eta} = -\mathbf{M}_{pp}\ddot{\mathbf{u}}_p - \mathbf{M}_{p\eta}\ddot{\boldsymbol{\eta}} - \mathbf{K}_{p\eta}\boldsymbol{\eta} \quad (18)$$

In order to combine BEM for a liquid region and FEM for a structure region, the nodal displacement vector ( $\mathbf{u}$ ) in Eq. (9) is divided into the displacement vector of fluid-structure interface nodes ( $\mathbf{u}_p$ ) and the structural nodes only ( $\mathbf{u}_o$ ). The governing equation of the liquid-structure interaction system is obtained by using the compatibility and equilibrium conditions at the interface. This superstructure system is superimposed on a base isolation system modeled by the hysteretic element presented in above section. The equations of motion for the superstructure and base can be formulated by introducing the relative displacement vector with respect to the base. Combining these equations results in the following;

$$\begin{bmatrix} \mathbf{M} & \mathbf{Mr} \\ \mathbf{r}^T \mathbf{M} & \mathbf{r}^T \mathbf{Mr} + \mathbf{m}_b \end{bmatrix} \begin{Bmatrix} \ddot{\mathbf{v}} \\ \ddot{\mathbf{v}}_b \end{Bmatrix} + \begin{bmatrix} \mathbf{C} & 0 \\ 0 & \mathbf{c}_b \end{bmatrix} \begin{Bmatrix} \dot{\mathbf{v}} \\ \dot{\mathbf{v}}_b \end{Bmatrix} + \begin{bmatrix} \mathbf{K} & 0 \\ 0 & \mathbf{k}_b \end{bmatrix} \begin{Bmatrix} \mathbf{v} \\ \mathbf{v}_b \end{Bmatrix} = - \begin{bmatrix} \mathbf{Mr} \\ \mathbf{r}^T \mathbf{Mr} + \mathbf{m}_b \end{bmatrix} \begin{Bmatrix} \ddot{\mathbf{u}}_g \end{Bmatrix} - \begin{Bmatrix} \mathbf{K}^l \cdot \mathbf{A} \\ 0 \end{Bmatrix} - \begin{Bmatrix} 0 \\ \mathbf{c} \end{Bmatrix} \quad (19)$$

where

$$\mathbf{M} = \begin{bmatrix} \mathbf{M}_{oo}^s & \mathbf{M}_{op}^s & \mathbf{0} \\ \mathbf{M}_{po}^s & \mathbf{M}_{pp}^s + \mathbf{M}_{pp}^l & \mathbf{M}_{p\eta}^l \\ \mathbf{0} & \mathbf{M}_{\eta p}^l & \mathbf{M}_{\eta\eta}^l \end{bmatrix}, \mathbf{C} = \begin{bmatrix} \mathbf{C}_{oo}^s & \mathbf{C}_{op}^s & \mathbf{0} \\ \mathbf{C}_{po}^s & \mathbf{C}_{pp}^s + \mathbf{C}_{pp}^l & \mathbf{C}_{p\eta}^l \\ \mathbf{0} & \mathbf{0} & \mathbf{C}_{\eta\eta}^l \end{bmatrix}, \mathbf{K} = \begin{bmatrix} \mathbf{K}_{oo}^s & \mathbf{K}_{op}^s & \mathbf{0} \\ \mathbf{K}_{po}^s & \mathbf{K}_{pp}^s & \mathbf{K}_{p\eta}^l \\ \mathbf{0} & \mathbf{0} & \mathbf{K}_{\eta\eta}^l \end{bmatrix}, \mathbf{K}^l = \begin{bmatrix} \mathbf{0} & \mathbf{0} & \mathbf{0} \\ \mathbf{0} & \mathbf{K}_{pp}^l & \mathbf{K}_{p\eta}^l \\ \mathbf{0} & \mathbf{0} & \mathbf{K}_{\eta\eta}^l \end{bmatrix}$$

$$\mathbf{v} = [\mathbf{v}_o \quad \mathbf{v}_p \quad \boldsymbol{\eta}]^T, \dot{\mathbf{v}} = [\dot{\mathbf{v}}_o \quad \dot{\mathbf{v}}_p \quad \dot{\boldsymbol{\eta}}]^T, \ddot{\mathbf{v}} = [\ddot{\mathbf{v}}_o \quad \ddot{\mathbf{v}}_p \quad \ddot{\boldsymbol{\eta}}]^T, \mathbf{A} = [\mathbf{0} \quad \mathbf{A}_p \quad \mathbf{A}_\eta]^T$$

and  $\mathbf{m}_b$  is the mass matrix of the base,  $\mathbf{c}_b$  and  $\mathbf{k}_b$  are the resultant damping and stiffness matrix of the base isolation system, respectively, and  $\mathbf{c}$  is a vector containing the forces mobilized in the nonlinear elements of the isolation system.  $\ddot{\mathbf{v}}$ ,  $\dot{\mathbf{v}}$ , and  $\mathbf{v}$  represent the acceleration, velocity, and displacements vectors of the fluid-structure interaction system relative to the base, and  $\ddot{\mathbf{v}}_b$  is the vector of base acceleration relative to the ground

### Solution procedure of fully coupled system

In this paper, the solution of governing equations of motion for the whole system is obtained by the direct integration method in time domain. Using the solution procedure of non-linear sloshing motion, the initial value of a fluid region at each time step is achieved. Then, the whole system equation, Eq. (19) which is containing the non-linear term of the base isolation system is solved using the pseudo-force method and the responses of the structure and fluid regions are obtained. Those solution procedure involves following two stages: (1) Solution of the equation of motion using an unconditionally stable Newmark's average acceleration method; and (2) Solution of the differential equation governing the nonlinear behavior of the isolation elements using an unconditionally stable semi-implicit Runge-Kutta method suitable for stiff differential equations. Using those results as input data, the solution procedure of non-linear sloshing motion is repeated. Then, the initial and corrected values of free surface are compared. If a desired level of convergence is achieved for the sloshing motion of the fluid region, next time step begins. However, if a desired level of convergence is not achieved, the above procedure is repeated in a iterative manner.

## NUMERICAL ANALYSIS AND RESULTS

### Slosh response - forced lateral oscillation

To validate the developed numerical analysis algorithm, the non-linear behavior of the free surface in a rigid container is considered. The similar problem is solved by Kasuga et al. [7] and is available in the literature. The container is having a radius 0.5m and is filled with water up to a depth of 0.5m. It is subjected to a sinusoidal horizontal acceleration of the type given as

$$a_x(t) = D_x \omega^2 \sin \omega \cdot t \quad (20)$$

where  $D_x$  and  $\omega$  are the amplitude and the frequency of the forced horizontal displacement, respectively. In this analysis, the parameters of  $D_x$  and  $\omega$  are 0.01m and 5.85rps, respectively.

The analysis results for both linear and non-linear free surface boundary conditions are shown in Fig. 2 which shows the time history of the free surface displacement at  $x = R$ ,  $y = 0$  of the container. To verify the developed analysis program and study the effect of the non-linear free surface boundary condition, the present numerical results are compared with the solution of Kasuga et al. As shown in Fig. 2, the trend of the present results for non-linear boundary condition agrees well with those of Kasuga et al. in respect of the amplitude and periodicity of the response. It may be observed that there is an upward shifting of the amplitude due to the effect of non-linear boundary condition.

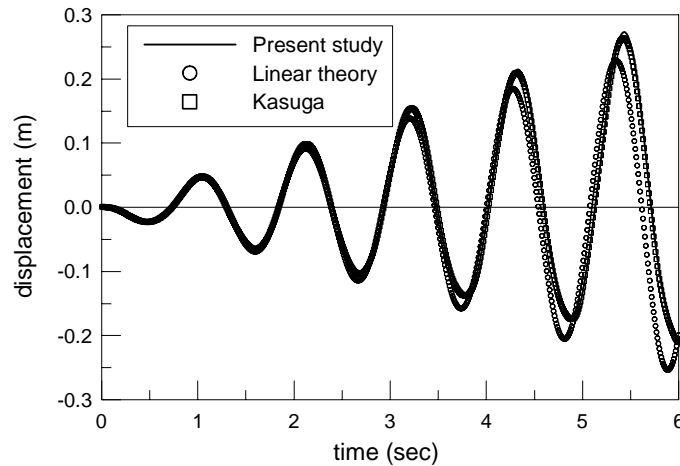


**Fig. 2 Free surface displacements due to horizontal forced vibration**

### Fluid-structure interaction considering the non-linear free surface boundary condition

A seismic analysis is performed to investigate the effect of the non-linear free surface boundary condition on the behavior of a liquid storage tank. The dimensions of the liquid storage tank is  $R$  (radius)=7.32m,  $H$  (height)=21.96m, and  $t$  (wall thickness)=0.0254m. The liquid container is filled with water up to a depth of 21.96m. The material properties for the tank are Young's modulus  $E=206.70\text{GPa}$ ; Poisson's ratio  $\nu=0.3$ ; and density  $\rho_s=7,840\text{kg/m}^3$ . The north-south component of the 1940 El Centro earthquake records, with a peak acceleration of 0.348g, is used as the input ground acceleration into the horizontal direction. Damping ratios for the structure-impulsive interaction part and the sloshing interaction part are assumed to be 2% and 0.5%, respectively.

Fig. 3 represents time histories of the sloshing displacement and base overturning moment for linear and non-linear boundary conditions, respectively. Table 1 summarized the maximum responses to the earthquake. From the analysis results, the maximum radial displacement and resultant forces are not seriously affected by the free surface boundary condition. Fig. 3(a) shows that the sloshing displacement of a free surface increases thoughtfully when the non-linear boundary condition is applied.

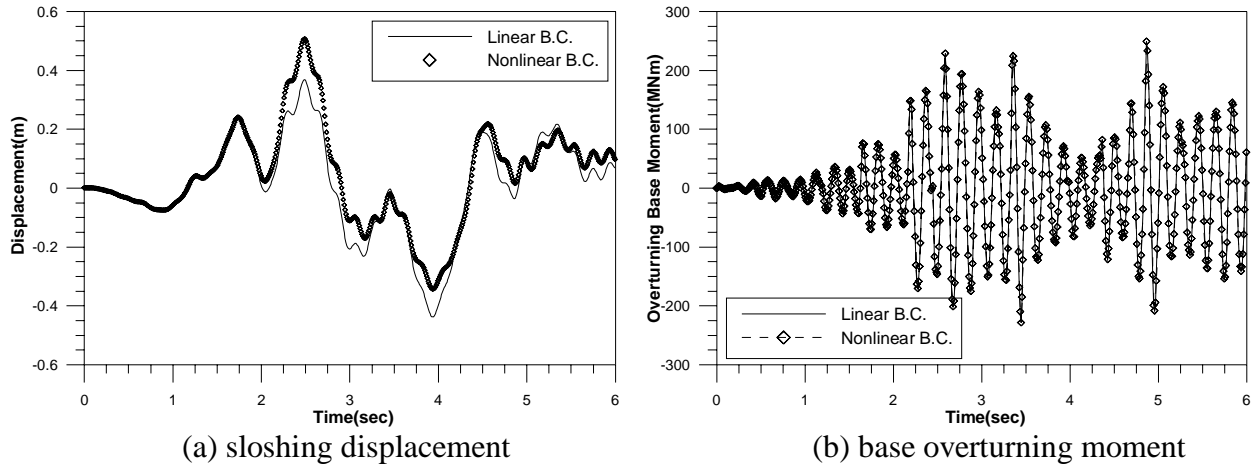


**Fig. 3 Time history of seismic response of a liquid storage tank**

**Table 1 Response of a liquid storage tank for linear and non-linear boundary conditions**

SI Unit	Linear case		Non-linear case	
	Value	Time(sec)	Value	Time(sec)
$v_{s \max} (cm)$	1.080	2.68	1.081	2.68
$M_{\max} (Nm)$	$2.495 \times 10^8$	4.87	$2.493 \times 10^8$	4.87
$Q_{\max} (N)$	$2.111 \times 10^7$	4.87	$2.109 \times 10^7$	4.87
$N_{\max} (N/mm)$	$1.482 \times 10^6$	4.87	$1.481 \times 10^6$	4.87
$\eta_{\max} (cm)$	36.80	2.49	50.63	2.49

**Seismic response of a base isolated LNG tank for various liquid depths**

A seismic fluid-structure-base isolation interaction analysis for the real size LNG tank is performed to evaluate the applicability of the developed method. The dimensions of the LNG tank is  $R=43.0m$ ,  $H$  (including the wall and roof)= $44.0m$ , and  $t=0.75m$ . The liquid container is filled with LNG up to various depths; full, 3 quarters, half and 1 quarter. The material properties for the tank are  $E=26.0GPa$ ,  $\nu=0.2$  and  $\rho_s=2,500kg/m^3$  and the properties of the isolator are  $\alpha=0.15$ ,  $F^y=6900KN$  and  $Y=0.65cm$ . The artificial earthquake with a peak acceleration of  $0.2g$  is used as the input ground motion into the horizontal direction. Damping ratios for the structure-impulsive interaction part and the sloshing interaction part are assumed to be 2% and 0.5%, respectively.

Fig. 4 represents the sloshing displacements of linear and non-linear boundary conditions for various liquid depths. Table 2 summarized the maximum responses to the earthquake. From the results, the base isolation increases the liquid sloshing displacement considerably. However, the structural responses such as a radial displacement, base shear, overturning moment are reduced effectively. Those trends become more severe with increasing liquid depth.

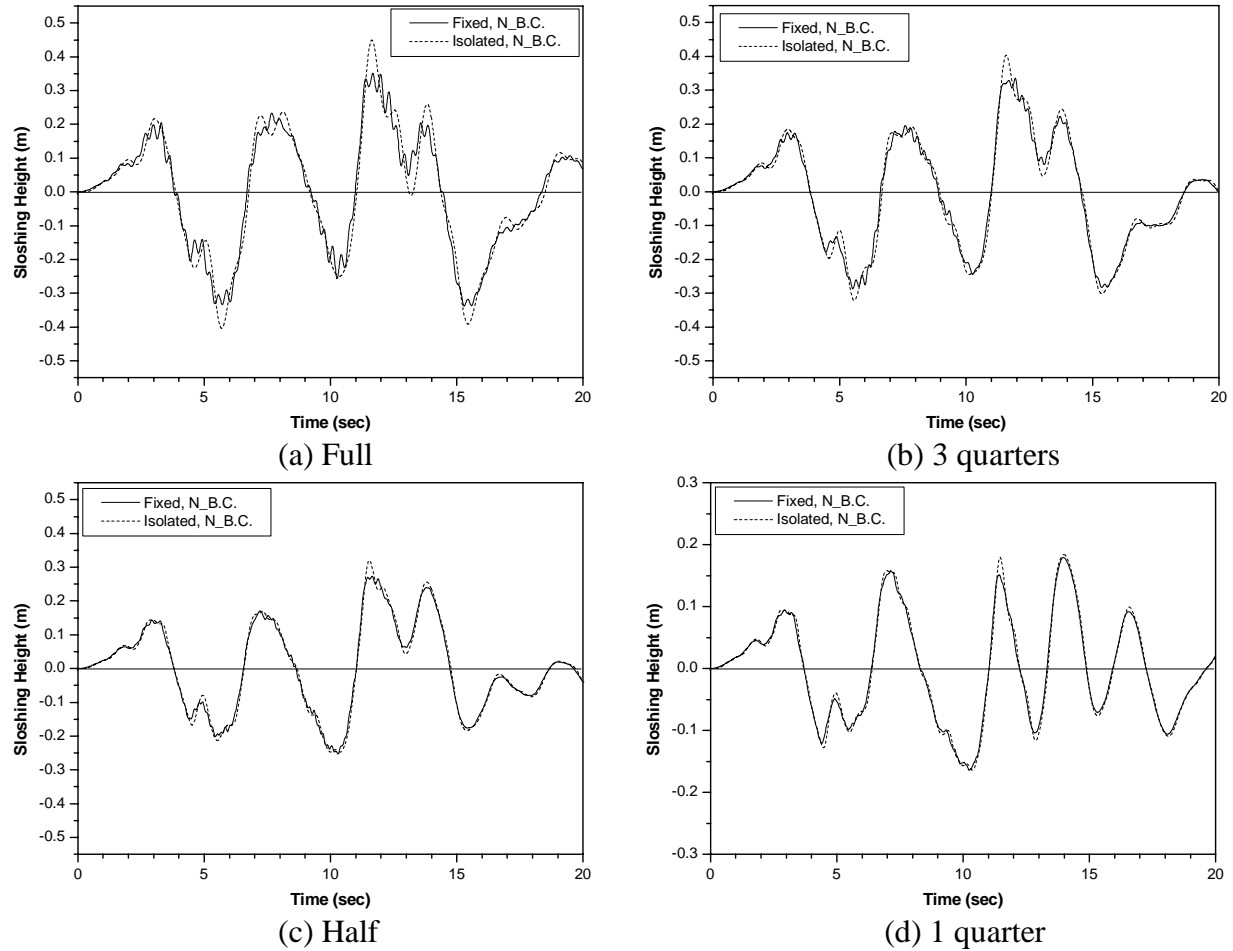


**Fig. 4 sloshing height of free surface for various liquid depths**

**Table 2 Response of a base isolated LNG tank for various liquid depths**

			$v_{s,max} (cm)$	$M_{max} (Nm)$	$Q_{max} (N)$	$\eta_{max} (cm)$
Full	Fixed	Value	0.836	$5.91 \times 10^9$	$4.33 \times 10^8$	35.1
		Time(sec)	12.17	12.17	12.17	11.69
	Isolated	Value	0.161	$1.35 \times 10^9$	$8.35 \times 10^7$	44.9
		Time(sec)	11.6	5.69	5.69	11.63
3 Quarters	Fixed	Value	0.280	$2.71 \times 10^9$	$2.54 \times 10^8$	33.5
		Time(sec)	11.98	6.15	6.15	11.96
	Isolated	Value	0.087	$6.37 \times 10^8$	$5.31 \times 10^7$	40.3
		Time(sec)	11.52	11.47	11.47	11.59
Half	Fixed	Value	0.190	$5.89 \times 10^8$	$8.08 \times 10^7$	27.2
		Time(sec)	11.01	5.69	5.69	11.66
	Isolated	Value	0.081	$2.65 \times 10^8$	$3.38 \times 10^7$	32.1
		Time(sec)	11.45	11.47	11.47	11.54
1 quarter	Fixed	Value	0.188	$5.24 \times 10^7$	$1.25 \times 10^7$	17.9
		Time(sec)	7.73	11.31	11.31	13.97
	Isolated	Value	0.073	$4.21 \times 10^7$	$1.01 \times 10^7$	18.4
		Time(sec)	11.45	11.45	11.45	13.99

## CONCLUSIONS

The numerical analysis of base isolated liquid storage tanks subjected to a dynamic loading is examined using the coupling method, which combined the finite elements for a structure region and a base isolation system and the boundary elements for a fluid region. To evaluate the effect of a fluid-structure interaction accurately, the non-linear boundary condition of a free surface is considered. The procedure developed in this study is concentrated on a cylindrical storage tank; however, it is applicable to other tank configurations because no geometric assumption or simplification is included in it. Through this study, following results are obtained.

(1) To validate the developed numerical algorithm, Results of present study for forced horizontal vibration is compared with those of linear analysis and Kasuga et al. The forced vibration analysis demonstrates that the developed method can represent the large sloshing motion of free surface. Also, as the effect of non-linearity becomes large, the shape of free surface motion is changed to a non-symmetric configuration and the upward displacement is considerably enlarged.

(2) Fluid-structure interaction analysis is performed for a seismically excited liquid storage tank considering both the linear and non-linear free surface boundary conditions. Then, the fact that the maximum sloshing height is less estimated by the analysis using the linear free surface boundary condition is found out. Also, it can be found that the maximum radial displacement and stress resultants of the structure and hydrodynamic pressure acting on the wall are not seriously affected by the free surface boundary condition.

(3) To evaluate the applicability of the developed method, a numerical analysis of a base isolated LNG tank is performed for the different liquid levels. From the results, the base isolation increases the liquid sloshing displacement considerably. However, the structural responses such as a radial displacement, base shear, overturning moment are reduced effectively. Those trends become more severe with increasing liquid depth.

## REFERENCES

1. Stoker J.J. "Water Waves." Interscience Publishers, New York, 1954.
2. Longuet-Higgins M.S., Cokelet E.D. "The deformation of steep surface waves on water(1)." A Numerical Method of Computation, 1976; A350: 1-26.
3. Nakayama T. "Boundary element analysis of nonlinear water wave problems." International Journal of Numerical Methods in Engineering, 1983; 19: 953-970.
4. Lay K.S. "Seismic coupled modeling of axisymmetric tanks containing liquid." Journal of Engineering Mechanics, 1993; 119: 1747-1761.
5. Tsopelas P.C., Constantinou M.C., Reinhorn A.M.. "3D-BASIS-ME: Computer program for nonlinear dynamic analysis of seismically isolated single and mutiple structures and liquid storage tanks." In: Technical Report NCEER-94-0010, National Center for Earthquake Engineering Research, 1994.
6. Park Y.J., Wen Y.K., Ang A.H.S. "Random vibration of hysteretic systems under bidedctional ground motions." Earthquake Engineering and Structural Dynamics, 1986; 14(4): 543-557.
7. Kasuga L., Sugino, R., Tosaka, N. "Sloshing motion in a cylindrical container by boundary element method," Boundary Element Methods, Eds. M. Tanata, Q. Du and T. Honma, Elsevier, 1993: 315-324.